STRATEGIES

FOR FUTURE CLIMATE RESEARCH

STRATEGIES FOR FUTURE CLIMATE RESEARCH*)

Edited by Mojib Latif

*)A collection of papers presented at the birthday colloquium in honour of Klaus Hasselmann's 60th anniversary.

Max-Planck-Institut für Meteorologie
Bundesstraße 55
D-2000 Hamburg 13

One Example of a Natural Mode of the Ocean Circulation in a Stochastically Forced Ocean General Circulation Model

Uwe Mikolajewicz and Ernst Maier-Reimer

Abstract

One dominating example of the variability occurring in an OGCM forced with white noise fresh water fluxes is analyzed with the POP-method. It has a period of 330 years and strongly affects deep water formation, atmosphere-ocean heat exchange and the thermohaline circulation. The sensitivity to the amplitude of forcing and the formulation of the equation of state is discussed.

1. Introduction

One of the major difficulties in the problem of detecting climate changes induced by anthropogenic greenhouse gases in the presence of natural climate variability is the estimation of the natural noise spectrum (Hasselmann, 1979). Though time series of appropriate length of climate parameters are sparse, it is known that this spectrum has significant power in the relevant frequency range of decades to a few centuries (Gates, 1985). Reviews of known time series have been given by Lamb (1977), Folland et al. (1990) and Crowley and North (1991).

For a reliable discrimination between man-made and natural fluctuations the complete spectrum of covariance in the time range under consideration must be known. Due to the sparseness of the available data, it is not possible to derive this from historical observations alone. The only feasible way to obtain estimates of the natural covariance spectra now is to augment the available observations by simulations with climate models. Since such lengthy simulations with fully coupled atmosphere-ocean-ice models are at present prohibitively expensive[1], we investigate in this paper the natural variability

[1] Up to now, results from coupled atmosphere-ocean general circulation models have been published describing simulations of up to 100 year length (Stouffer

with an ocean general circulation model (OGCM). On time scales of decades to a few centuries the ocean is believed to govern the structure of the probability spectrum through its internal dynamics and through the integration of short term atmospheric fluctuations, and it transforms the essentially white noise forcing into a red response spectrum (Hasselmann 1976).

Although the importance of the ocean for climate fluctuations has been known for a long time (e.g. v.Humboldt 1845), knowledge about regional details and dynamics of such long-term oscillations is still rather poor[2]. Several authors (e.g. Stommel 1961 or Rooth 1982) have argued that the different nature of heat and freshwater fluxes contributing to the net surface buoyancy flux may lead to slow oscillations between two different metastable states. This hypothesis has found support by experiments with the Princeton OGCM (Bryan 1986), by further theoretical investigations of Marotzke et al. (1988) and by results from a coupled atmosphere-ocean general circulation model (Manabe and Stouffer 1988). Simplified models of such behavior have been summarized by Welander (1986).

The importance of ocean-atmosphere feedbacks combined with the possible existence of different metastable circulation modes for climate change has been stressed in several papers concerned with the Younger Dryas event, the most important climatic fluctuation since the last deglaciation (e.g. Berger and Vincent 1986 or Broecker et al. 1988). Maier-Reimer and Mikolajewicz (1989) showed by sensitivity studies with an OGCM that it is possible, from a dynamical point of view, to produce Younger Dryas like events by meltwater input.

Recently Broecker et al. (1990) proposed the existence of a salt oscillator in the glacial Atlantic which might be responsible for the oscillations with a typical period of 2500 years found in the glacial part of $\delta O18$ records from Greenland ice cores (e.g. Dansgaard et al. 1984). The oscillator consists of a chain of feedback mechanisms between the two modes of the Atlantic circulation

---

et al. 1989, Cubasch et al. 1991).

[2] An exception is the El Niño/Southern Oscillation phenomenon, which has been studied extensively (e.g. Rasmusson and Carpenter 1982), but the typical time scale of this process (3 to 5 years) is probably too short to have serious effects for greenhouse detection studies.

- and the large difference in northward oceanic heat transport connected with them - and the growth or melting of northern hemispheric ice sheets.

Müller and Willebrand (1985) have reported the possibility of another form of "caballing" oscillation arising from the dependence of compressibility on temperature, with a relatively long oscillation period which is related to the time scale of vertical advection. So far, however, there is no experimental evidence of the existence of any of the oscillations described above in the real ocean. Rossby waves are presumably not slow enough to affect the low frequency part of the spectrum with which we are concerned.

The need for an investigation of such phenomena in realistic circulation models is emphasized by the simplifications underlying many of these theoretical approaches. In this paper we study the variability of an OGCM in response to a prescribed white noise atmospheric forcing. In the high frequency range of the variability spectrum, the ocean acts as a straightforward integrator without feedback, yielding an ω^{-2} red noise response spectrum. For lower frequencies ω, the details of the internal dynamics of the ocean determine the response, and the spectrum can be expected to be more complex (Hasselmann 1976). In the past, most stochastic forcing models have been formulated for relatively simple linear feedback systems allowing analytical or semi-analytical solutions, for example Lemke (1977), Wigley and Raper (1990) for the global ocean, Frankignoul and Hasselmann (1977), Reynolds (1979), and Herterich and Hasselmann (1987) for the surface ocean layers or Lemke et al. (1980) for sea ice. For the global ocean such simple models provide useful estimates of the expected orders of magnitude of oceanic variability but are incapable of capturing possible ocean oscillation modes which could yield strong amplifications in some parts of the variability spectrum and which might have a strong influence on climate variability.

We shall describe an experiment in which the Hamburg Large-Scale-Geostrophic OGCM is driven by climatological boundary values of temperature, fresh water and momentum fluxes with a superimposed fresh water flux noise. The noise is represented as a white noise forcing, i.e. with no correlation from month to month (the model time step) but with coherent spatial structures of approximately 25° correlation scale. The ocean response spectrum is found to have a pronounced peak around slightly more than 300 years which can be

identified with an "eigenmode" of the ocean. Some preliminary results from this experiment have been presented in Mikolajewicz and Maier-Reimer (1990).

2. The model and its initialization

The Hamburg Large-Scale-Geostrophic OGCM, whose concept was originally proposed by Hasselmann (1982), is especially designed for the study of slow climatic variations. An implicit integration method permits a time step of 30 days, thus allowing integrations over thousands of years at acceptable computing cost. Basic features of this model are described in Maier-Reimer and Hasselmann (1987). Details are presented in Maier-Reimer et al. (1991), who discussed the sensitivity of the steady state ocean circulation to different formulations of the upper boundary condition for heat and salt. From a series of experiments with varying boundary conditions a standard run was defined which best reproduces the observed large-scale thermohaline circulation.

The model is based on the conservation laws for heat, salt and momentum (the latter in a linearized form), the full equation of state and the hydrostatic approximation. The present version of the model has a horizontal resolution of 3.5 x 3.5 degree and 11 vertical layers (centered at depths of 25, 75, 150, 250, 450, 700, 1000, 2000, 3000, 4000 and 5000 m). Topography is included, as well as a one-layer thermodynamic sea ice model with viscous rheology. The annual cycle is resolved in the model, although in this paper only annual mean values will be shown.

For the momentum flux forcing at the upper boundary the monthly mean wind stress climatology of Hellerman and Rosenstein (1983) was used. The temperature in the surface layer was computed by a Newtonian type coupling to prescribed monthly mean air temperatures derived from the COADS data set (Woodruff et al., 1987), with a coupling coefficient of 40 $Wm^{-2}K^{-1}$ (in the absence of sea ice). This yields a time constant of approximately 2 months for a surface layer thickness of 50m.

In a first initialization run[3], the model was driven with a similar Newtonian coupling (with a coupling coefficient of $1.5x10^{-5}$m/s) to the

[3] Run ATOS1 from Maier-Reimer et al. (1991)

observed climatological annual mean surface salinity (Levitus 1982). As initial condition, homogeneous water with a potential temperature of 2.5°C and with a salinity of 34.5 °/oo was used. After 10,000 years of integration this run had achieved an almost stationary state with a residual trend of less than $2x10^{-6}$K/year for potential temperature and $5x10^{-8}$ °/oo/year for salinity in the 4000 m layer. From this run, the effective freshwater flux arising from the coupling to the observed salinity was determined.

In the following experiments, this freshwater flux was then taken as boundary forcing acting on the surface salinity (and on the surface elevation), while still retaining the relaxation to the prescribed atmospheric temperature as the temperature boundary condition.

In the absence of a coupled atmospheric model, these "mixed" boundary conditions may be regarded as a reasonable approximate description of the feedback between the ocean and the atmosphere. Anomalies of the sea surface temperature (SST) are damped out by the resultant anomalous atmosphere-ocean heat fluxes, whereas anomalies in the surface salinities have no influence on the net fresh water flux. Thus anomalies in the salinity distribution have much longer lifetimes than anomalies of the SST as indicated by observations[4].

This simple atmosphere must be expected to give reasonably realistic results for small disturbances, but whether or not it yields a sufficiently realistic response for large changes in the ocean circulation is difficult to prove. At least in one case it is possible to compare results using this type of boundary condition (Maier-Reimer and Mikolajewicz 1989) with results from a coupled atmosphere-ocean general circulation model (Manabe and Stouffer 1988). Both models have shown the existence of a second steady state for the thermohaline circulation of the Atlantic with completely reversed Atlantic circulation. So there are some reasons to believe that results obtained with this type of boundary condition are realistic, at least in a qualitative

---

[4] A convincing example for the lack of atmospheric feedback on the salinity was observed in the seventies, when a large negative salinity anomaly in the Northern Atlantic persisted for at least 14 years (Dickson et al. 1988). Frankignoul and Hasselmann (1977) gave an estimate of 6 months for the typical lifetime of North Pacific SST anomalies from the calibration of a stochastic climate model.

sense.

In a second stage of initialization the model was started from an initial state given by the stationary field from the first initialization run and integrated further with prescribed, non-perturbed freshwater fluxes. After 4000 years of integration the model still exhibited the same circulation as in the first initialization run. This run will be referred to as the control run. The long integration time was needed to ensure that the circulation remained stable after the switch in the salinity boundary condition[5].

3. Description of the experiment

The short-term atmospheric fluctuations influence the ocean at the upper boundary in surface temperature, wind stresses and freshwater fluxes. Because of the lack of experience with such a complex stochastic climate model we decided to restrict ourselves to the oceanic response to fluctuations in one component only. From the study of the oscillators proposed in the literature (see introduction) and the lack of feedback mechanisms for the surface salinity we concluded that fluctuations in the freshwater flux were likely to be the most important contributor on time scales of decades and longer. The freshwater flux forcing applied was white in time, had a horizontal correlation of roughly 25° and a globally averaged standard deviation of 16mm/month. This value corresponds to 20% of the globally averaged annual mean precipitation (Baumgartner and Reichel 1975). A comparison with data from a 20 year AGCM-simulation forced with observed SST (W. König, personal comm.) shows that this value is reasonable for high latitudes, whereas it is a gross underestimation of the tropical variability.

For the construction of spatially coherent patterns of the freshwater flux we used an analogy of spherical harmonics, specified for the scalar product which is given by our topography. For this purpose we took the first thirty eigenfunctions of the Laplace operator in our grid with the boundary condition of vanishing gradients normal to coasts, as is appropriate for scalar

---

[5] Bryan (1986) and Marotzke (1990) have reported strong changes in the ocean circulation - up to a switch between the two modes of Atlantic thermohaline circulation - at this step of the initialization process.

quantities. The eigenfunctions were obtained by a repeated application of the Ritz procedure, which yields a series of eigenvalues in ascending order. The structures in the open ocean are similar to those of spherical harmonics. All eigenfunctions were used with equal weights.

In the open ocean the standard deviation of the net freshwater flux is almost constant at a level of 15 mm/month. Towards the coasts the amplitude generally increases. The largest amplitudes are seen in the almost closed basins of Hudson Bay and the Mediterranean (fig. 1). Despite the large variations obtained by this noise forcing, the long term mean state of the circulation remained remarkably close to the state of the control run.

The locations of deep water formation are shown in fig. 2. Deep water formation is indicated by the time rate of loss of potential energy due to application of the convective adjustment procedure. The region of strongest deep water formation is the North Atlantic. Most of the North Atlantic deep water is formed in the Irminger Sea and not in the Arctic, as it probably should be. In the Southern Ocean, the main source of deep water is the Weddell Sea, but there are many other regions where deep convection takes place.

Fig. 3 shows the zonally integrated meridional mass transport stream function of the Atlantic. (The lack of meridional boundaries makes this quantity meaningless south of 30°S.) The basic feature of the Atlantic meridional flow is a northward inflow from the Southern Ocean of 17 Sverdrup (Sv) in the upper 1.5 km which sinks in the North Atlantic to form the North Atlantic deep water (NADW). The flow leaves the Atlantic at depths of 2 to 3 km. The deeper inflow of Antarctic bottom water (AABW) has a strength of 6 Sv. At the surface, wind driven Ekman cells are seen. This pattern of meridional overturning is consistent with the Atlantic segment of the global "conveyor belt" (Gordon 1986, see also Wüst 1933 and for the surface branch v. Humboldt 1845). From the analysis of data for temperature, salinity, nutrients and potential vorticity, Roemmich and Wunsch (1985) estimate a meridional thermohaline circulation of 17 Sv (at 24°S). Gordon and Piola (1983) give a value near 20Sv based on surface salinity and the freshwater flux climatology as given by Baumgartner and Reichel (1975).

The north-south section of salinity through the western Atlantic (fig. 4)

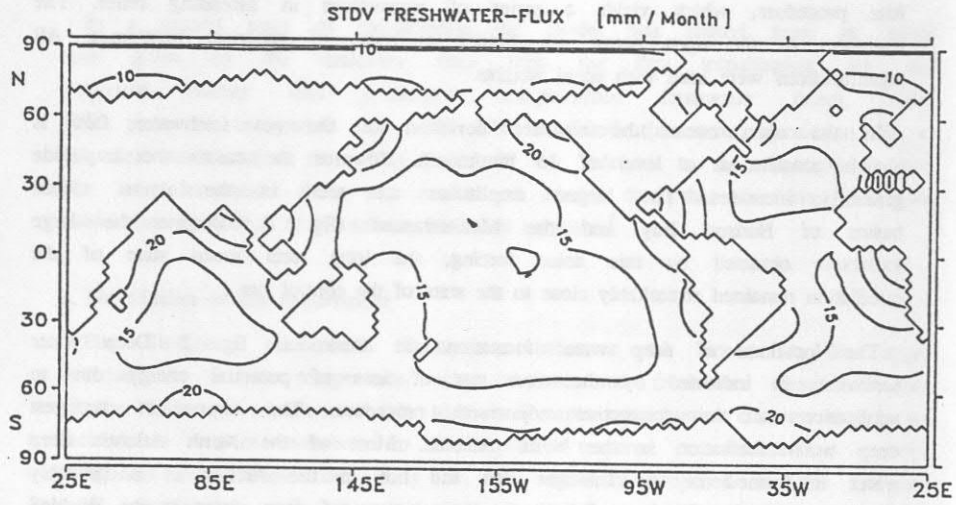

Fig. 1

Standard deviation of the noise added to the climatological fresh water flux.

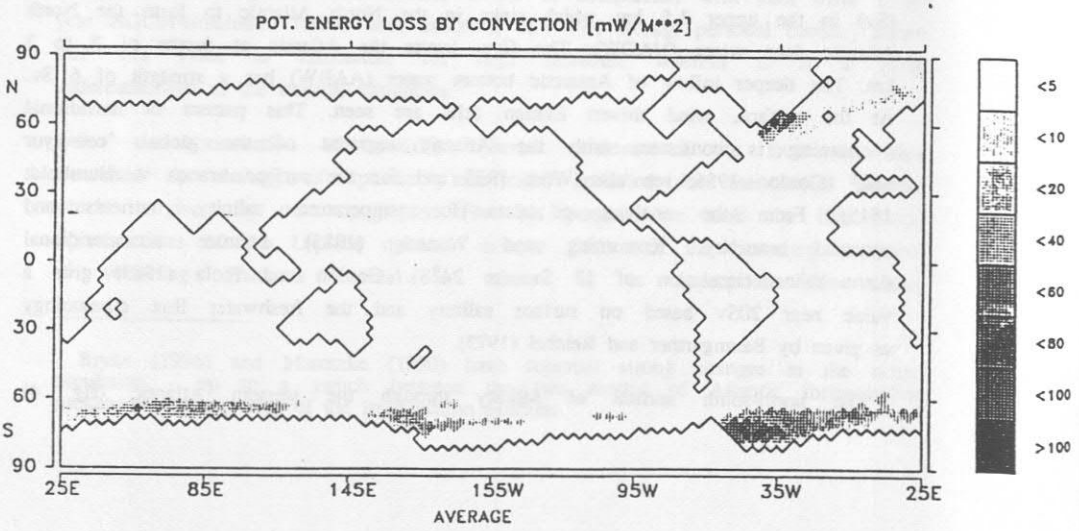

Fig. 2

Time rate of loss of potential energy due to convection averaged over the 3800 years of integration. This quantity gives an estimate of the effeciency of deep water formation in different locations.

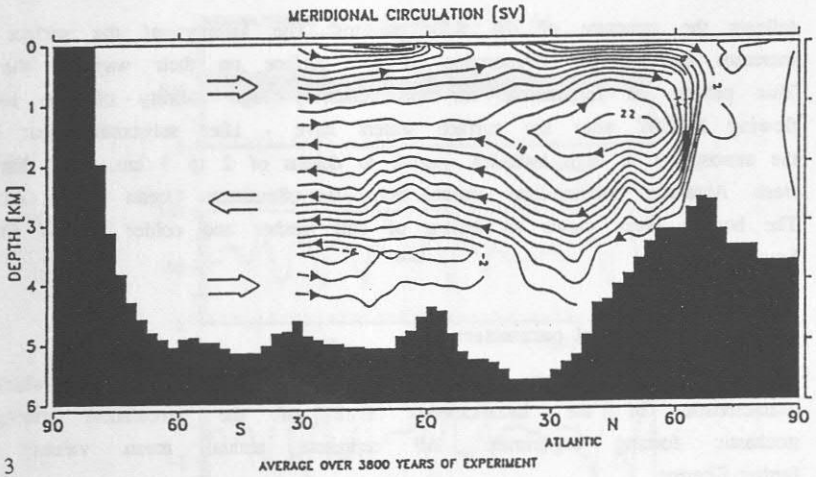

Fig. 3

Zonally integrated mean meridional mass transport streamfunction of the Atlantic averaged over the 3800 years of integration. Because of the lack of solid meridional boundaries south of 30°S this quantity is meaningless in these latitudes. The arrows indicate the direction of the flow, contour interval is 2 Sverdrup.

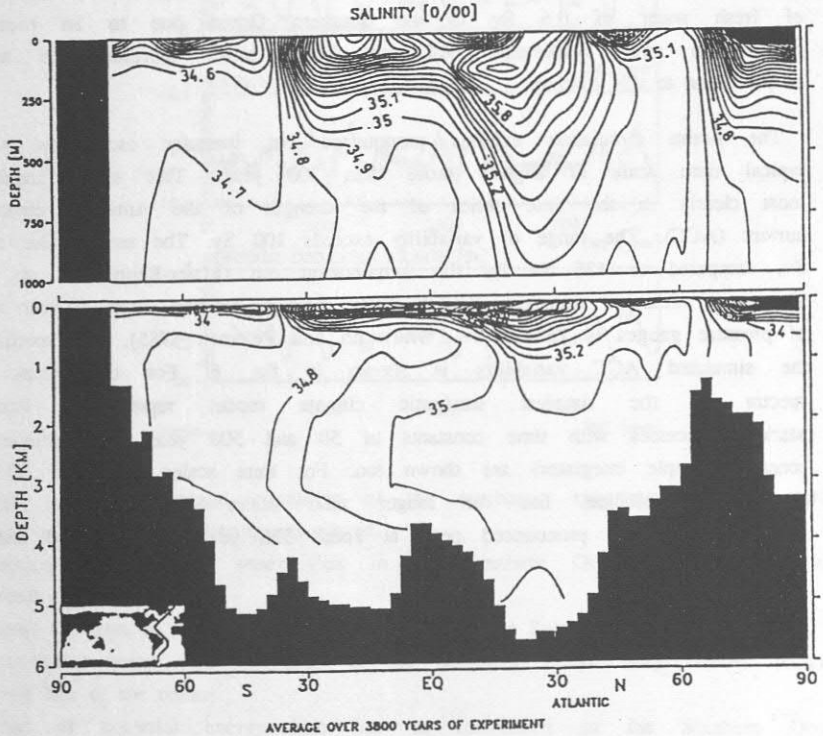

Fig. 4

Mean salinity (averaged over the 3800 years of the experiment) section through the western Atlantic. The exact location of the section is shown in the insert. The upper panel shows an enlargement of the upper 1000 m. The different water masses referred to as AABW, NADW and Antarctic Intermediate water (AAIW) are detectable. The contour interval is 0.1°/oo.

follows the structure of the flow patterns. The salinity of the surface waters increases due to net evaporation at the surface on their way to the north. This process is responsible for the relatively high salinity of the southward flowing NADW after the surface waters have - after substantial heat loss to the atmosphere at high latitudes - sunk to depths of 2 to 3 km. At 1 km depth, fresh Antarctic intermediate water from the Southern Ocean flows northward. The bottom layer shows an inflow of still fresher and colder AABW from the Southern Ocean.

4. Analysis of integral parameters

Fig. 5 shows time series of some integral parameters which are characteristic of the instantaneous state of the circulation during the stochastic forcing experiment. All represent annual mean values without further filtering.

The first panel shows a time series of the integral of the net freshwater flux over the entire ocean south of 30°S, a quantity prescribed by the forcing. The short term variability is dominant and the frequency spectrum (shown in fig.6) is white, as it should be. In the mean, there is a net gain of fresh water of 0.6 Sv in the Southern Ocean due to an excess of precipitation over evaporation. All other time series represent the response of the ocean to this forcing.

The ocean circulation exhibits pronounced but irregular oscillations with a typical time scale of slightly more than 300 years. This signal stands out most clearly in the time series of the strength of the Antarctic circumpolar current (ACC). The range of variability exceeds 100 Sv. The mean value is 118 Sv, compared to 126 Sv for the initialization run (Maier-Reimer et al. 1991). The mean measured transport through Drake passage inferred from 3 year records of pressure gauges is 123±10 Sv (Whitworth and Peterson 1985). The spectrum of the simulated ACC variability is shown in fig. 6. For comparison, three spectra of the simplest stochastic climate model representing first-order Markov processes with time constants of 50 and 500 years and infinite time constant (simple integrator) are shown too. For time scales less than 30 years all spectra coincide, but for longer time scales the spectrum for our simulation shows a pronounced peak at about 320 years. Between 30 and 300

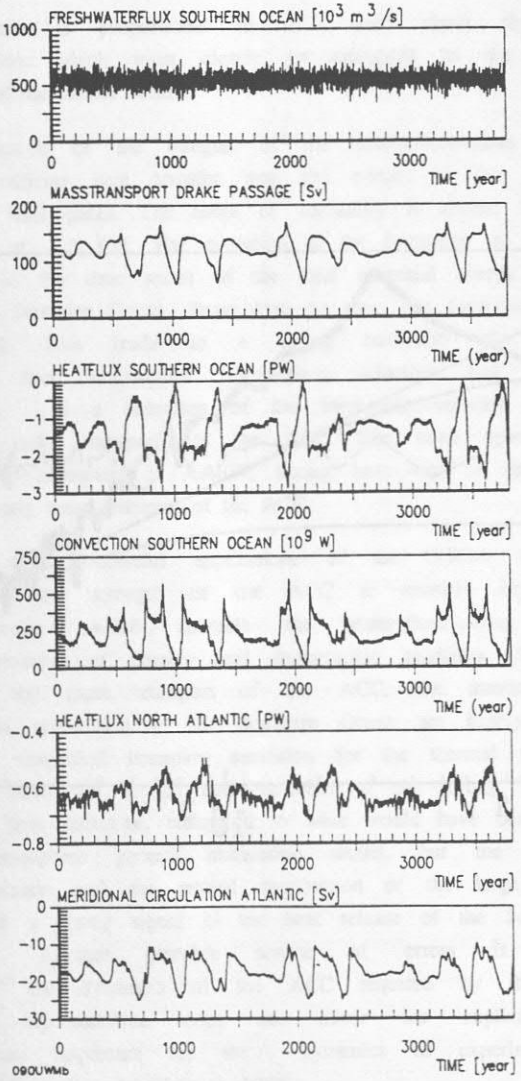

Fig. 5

Time series of integral quantities of the stochastic experiment. Annual mean values without further filtering are plotted.

- prescribed net fresh water flux in the Southern Ocean (all ocean points south of 30°S).
- mass transport of the ACC through Drake Passage (in Sv).
- atmosphere-ocean heat exchange in the Southern Ocean (neg. values indicate heat loss of the ocean).
- rate of potential energy loss due to convection in the Southern Ocean (measure of AABW formation).
- atmosphere-ocean heat exchange in the North Atlantic (north of 30°N) and Arctic ocean.
- zonally integrated masstransport stream function of the Atlantic at 30°S and 1500m depth indicating the strength of the NADW-outflow to the Southern Ocean.

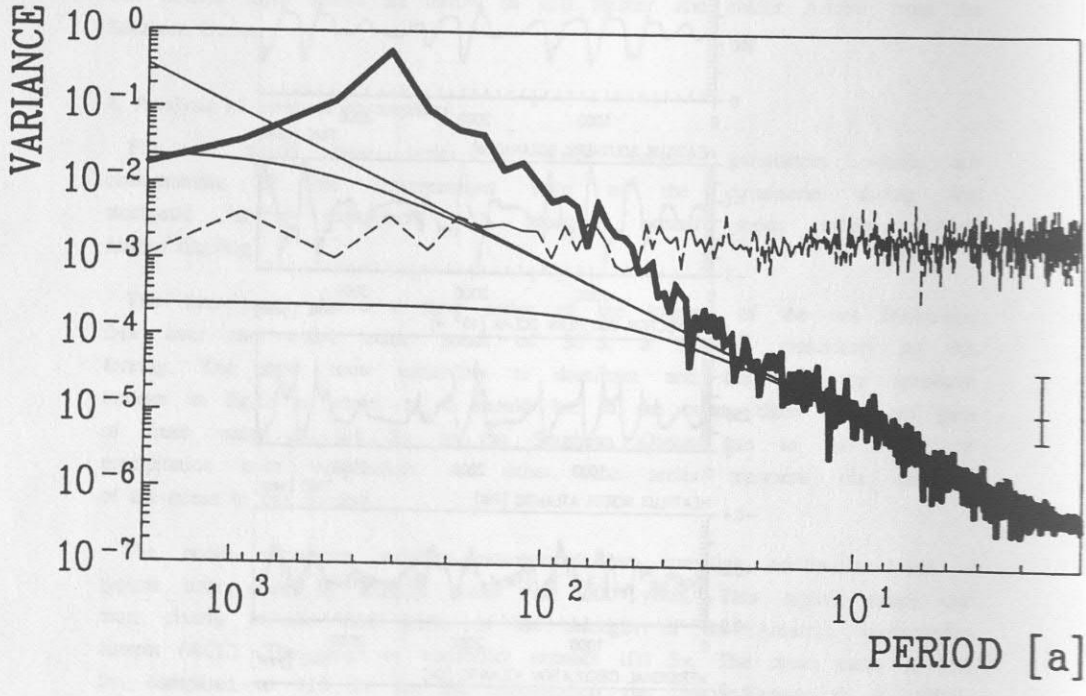

Fig. 6

Variance spectrum of the mass transport through Drake Passage and the net freshwater flux of the Southern Ocean (dashed line). Data are scaled by their standard deviation. The thin lines represent the results to be expected from simple stochastic climate models with a linear feedback term with time constants of 50 years, 500 years and infinite (corresponding to ω^{-2}), all fitted to the lower end of the ACC variance spectrum. For periods less than 30 years the shape of the spectrum can be approximated by such simple stochastic climate models, whereas for longer periods the spectral shape is significantly different due to the internal dynamics of the ocean, with a shape proportional to ω^{-3}. The bar indicates the 95% confidence interval.

years the spectrum is proportional to ω^{-3}, well above the simple ω^{-2} integrator, an effect which must clearly be attributed to the more complex internal dynamics of the model ocean.

The time evolution of the integral of the atmosphere-ocean heat exchange (positive values indicate heat transfer into the ocean) in the Southern Ocean is shown in the next panel. The range of variability is almost 3 PW compared to a mean value of -1.5 PW. The evolution of the formation of Antarctic bottom water is shown in the time series of the total potential energy release due to convection in the Southern Ocean. From time to time, the formation of AABW is totally suppressed. This leads to a strong reduction of the south-north density gradient, thus to weaker geostrophic velocities and - through the effect of friction - to a reduction of the barotropic velocity components and thus to reduced mass transports of the ACC. The same reasoning holds for episodes of strong formation of AABW, strong heat loss of the ocean to the atmosphere and strong mass transport of the ACC.

One of the first successful applications of an OGCM was indeed the demonstration that the strength of the ACC is strongly dependent on the temperature structure (which controls the atmosphere-ocean heat transfer) through the interaction of density and topographic gradients (Cox 1975). The time series of the mass transport of the ACC, the atmosphere-ocean heat exchange and the convection in the Southern Ocean are highly correlated with each other. The simplified boundary condition for the thermal forcing from the atmosphere may have led to an overestimation of the strong variations in the ocean-atmosphere heat exchange, compared to what would have been observed in a coupled ocean-atmosphere general circulation model, but the total cutoff of deep water formation and the related suppression of the large convective heat fluxes must yield a strong signal in the heat release of the Southern Ocean to the atmosphere. Another possible source of errors is the simplified representation of the dynamics of the ACC required by the coarse model resolution; this representation does not allow the explicit modeling of eddies, which are important for the dynamics as experiments with high resolution models show (e.g. Wolff et al. 1991).

The atmosphere-ocean heat exchange in the North Atlantic (north of 30°N including the Arctic) shows the same signal, though it is considerably weaker

and more noisy. The heat exchange in this region is inversely correlated with the heat fluxes of the Southern Ocean, indicating an inverse correlation between the formation of NADW and AABW. Consequently, the time series of the meridional stream function at 1500m depth at 30°S, an indicator of the strength of the outflow of NADW to the Southern Ocean, shows the same signal with a variability between 10 and 25Sv with maxima during episodes of weak AABW formation and strong formation of NADW.

The figures indicate that the ocean exhibits an "eigenmode" with a typical time scale of slightly more than 300 years which connects the polar regions and is asymmetric in the Atlantic with respect to the equator. The strongest effects are located around Antarctica. The thermohaline circulation of the Atlantic plays an important role. In this paper we will restrict ourselves to describing this particular mode as one example of long-term variability in the ocean. The mode does not appear as a continuous oscillation but rather in the form of discrete events, similar to El Niño.

5. Statistical analysis with the POP-method

To obtain more insight into the nature of the processes responsible for this oscillation, an analysis following the concept of principal oscillation patterns (POPs) was performed. This method was developed by Hasselmann (1988) and von Storch et al. (1988). It is the linearized and strongly simplified version of the more general principal interaction pattern (PIP, Hasselmann 1988) concept and has been designed especially for the simultaneous analysis of space-time variability. For a more detailed description of this method the reader is referred to the literature mentioned above or to von Storch et al. (1991, this volume).

Because of the direct effect of random fluctuations and the lack of a direct damping feedback mechanism for on the surface salinity, the salinity must be expected to be a key variable for the understanding of the eigenmode. From the analysis of the integral time series, it has become obvious that the thermohaline circulation of the Atlantic plays an important role in this process. Thus the anomalies of the salinity on the meridional section through the Western Atlantic (shown in fig. 4), which resembles the structure of the thermohaline circulation of the Atlantic, were used for the POP-analysis.

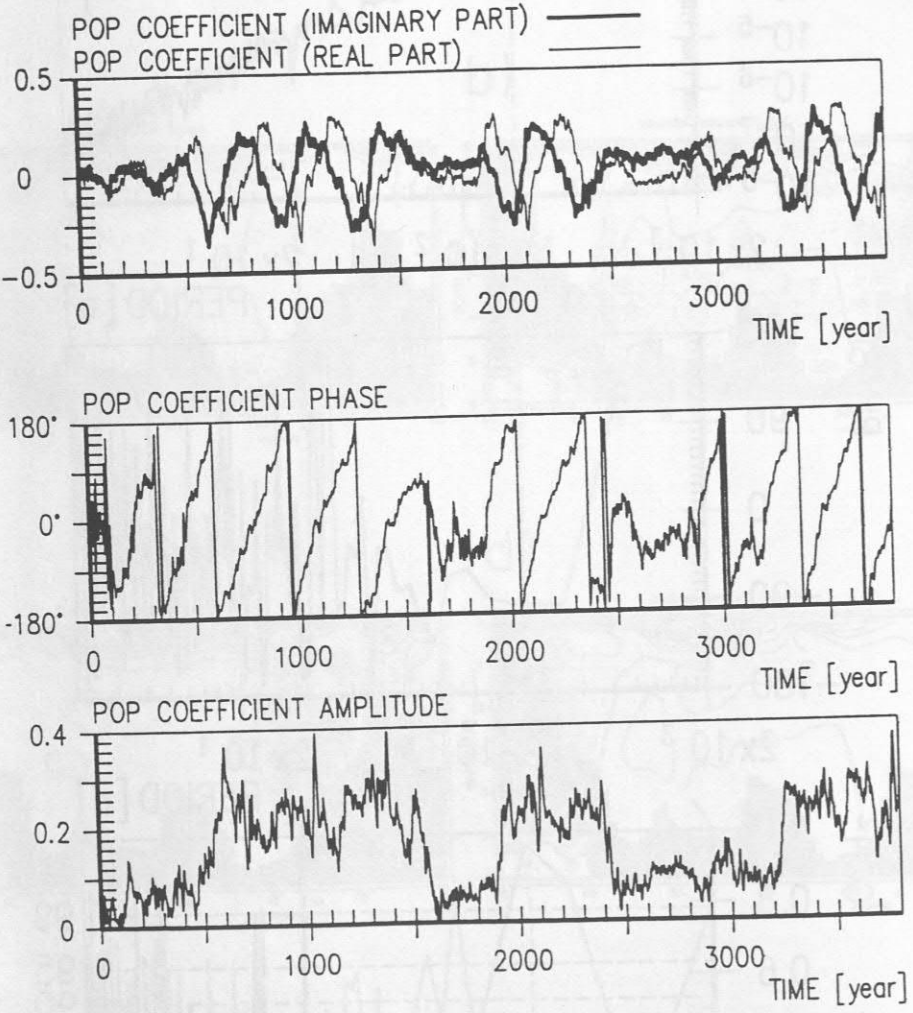

Fig. 7
Time series of components (a), phase (b) and amplitude (c) of the complex POP-coefficients.

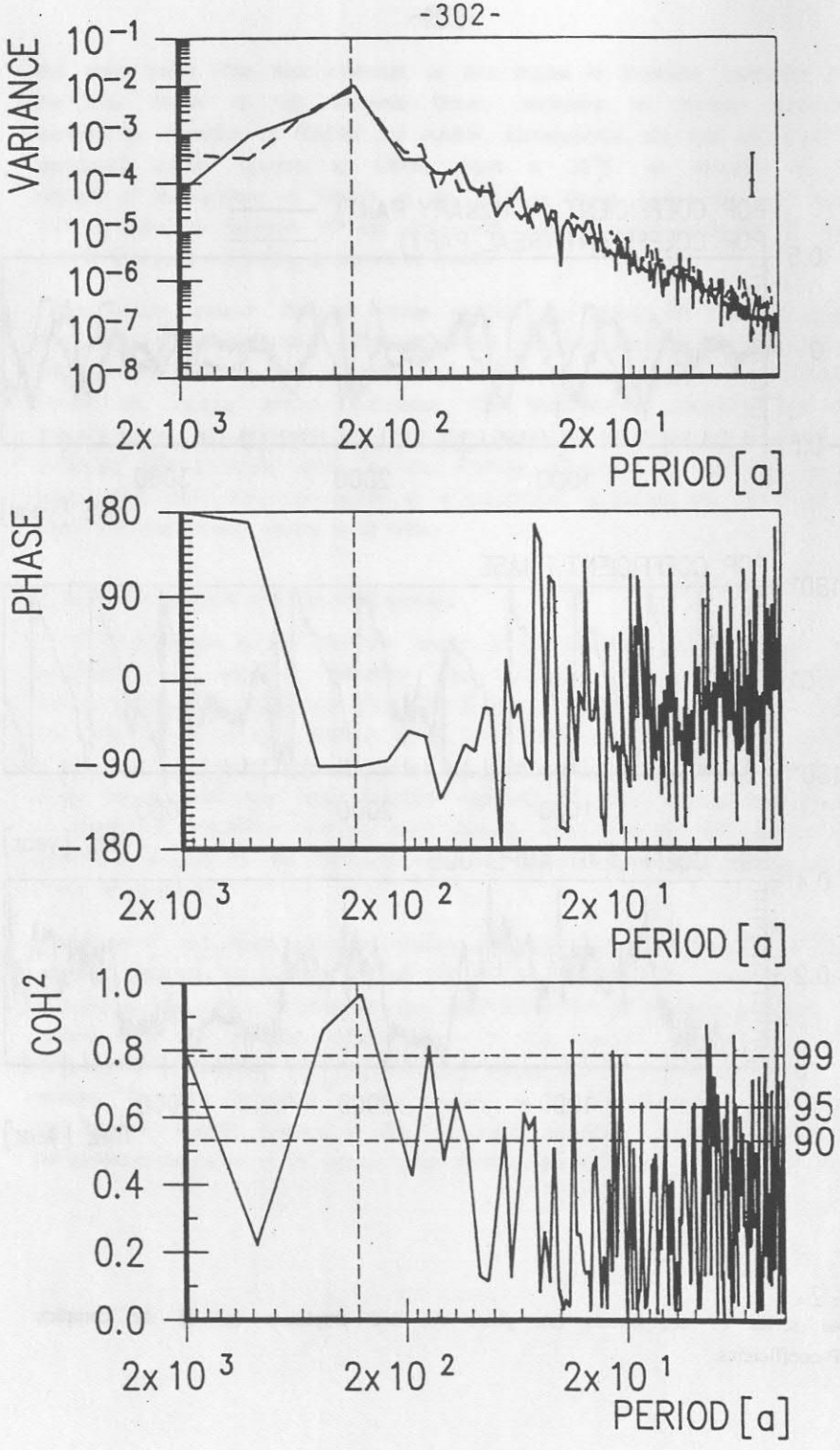

Fig. 8

Variance, phase and coherence spectra of the dominating POP.

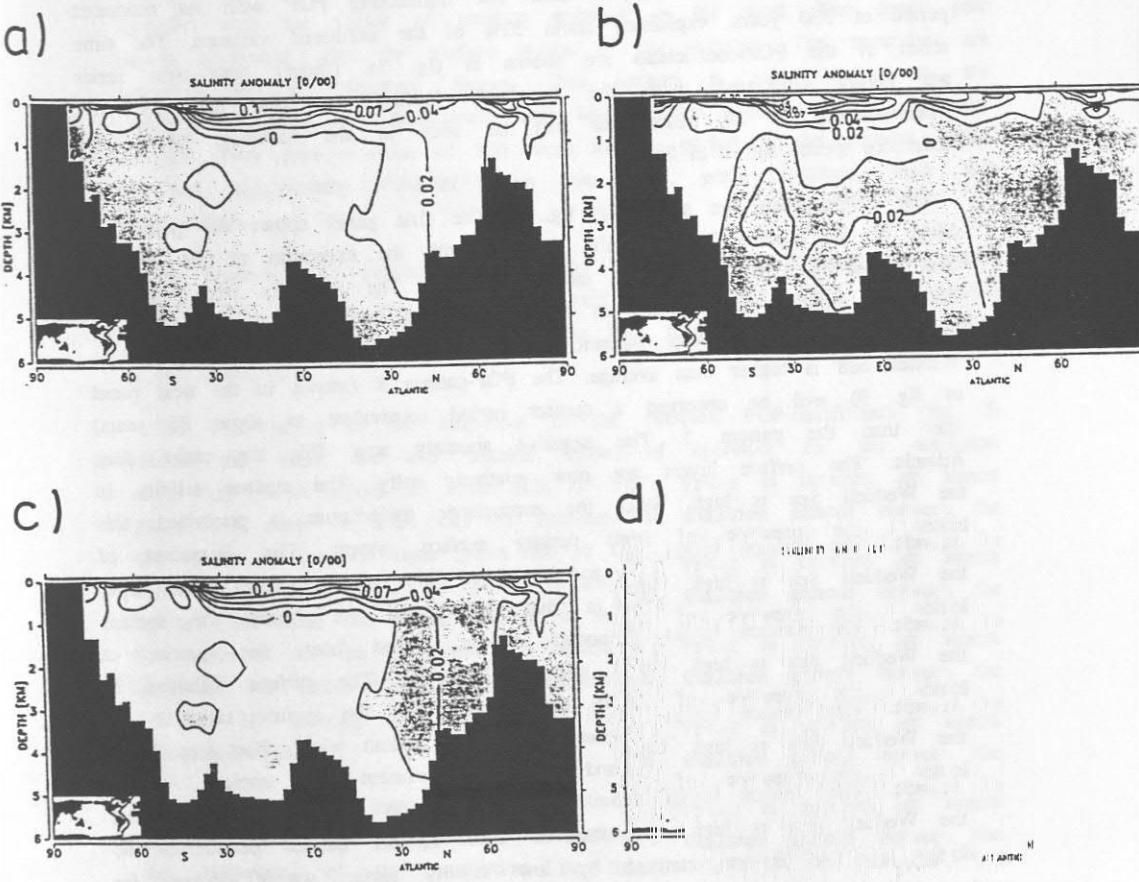

Fig. 9

POP-patterns 3, ℜ, -3, and -ℜ corresponding to salinity anomalies. Shading indicates negative values. The contour interval is variable. The patterns describe the propagation of salinity anomalies, each plot corresonding to the situation approximately 80 years apart.

The data from the experiment were stored as averages over 2 years. The stochastic fortcing resulted in a nonlinear response, which caused a slight model drift. To account for this, the linear trend was subtracted from the data. No further filtering was applied.

The results from this analysis show one dominating POP with an estimated period of 330 years, explaining about 52% of the unfiltered variance. The time series of the POP-coefficients are shown in fig. 7a. Clearly both time series are highly correlated, with the imaginary leading the real part by 90° (corresponding to 80 years), as can be seen in the variance, phase and coherence spectra shown in fig. 8.

The POP-patterns are shown in fig. 9. The first panel shows the pattern $\Im$. Most of the surface layer of the Atlantic, with the exception of the Weddell Sea, is occupied by a negative salinity anomaly. The relatively fresh water in the deep Atlantic is restricted to regions north of 30°N, whereas the salinity in the rest of the deep Atlantic together with the surface waters of the Weddell Sea is higher than average. The POP-pattern $\Re$ (shown in the next panel of fig. 9) will be observed a quarter period (equivalent to about 80 years) later than the pattern $\Im$. The negative anomaly now fills the entire deep Atlantic. The surface layers are now relatively salty. The surface salinity in the Weddell Sea is high. Since the atmospheric temperature is prescribed, this indicates the presence of high density surface waters. The formation of Antarctic bottom water is strong and associated with a large heat release from the ocean to the atmosphere in this region. In the Arctic the surface salinities are relatively low. Another quarter period later, the pattern $-\Im$ (the negative of the pattern $\Im$) will be observed. The surface salinities in the Atlantic are still high, but in the Weddell Sea the surface salinities are reduced and thus so is the formation of Antarctic bottom water. The deep North Atlantic is filled with saltier and the deep southern and tropical Atlantic with fresher water masses. A salinity distribution like pattern $-\Re$ (the negative of pattern $\Re$) will be observed about another quarter period (or 80 years) later. It is characterized by low salinity surfac waters (except for the northernmost parts of the Atlantic and the Arctic). The formation of Antarctic bottom water in the Weddell Sea is suppressed as indicated by the low surface salinities und thus low densities. The heat release from the ocean

to the atmosphere is small. The water masses in the deep Atlantic are distinctly saltier than usual. Another 80 years later the pattern 3, described in the beginning of this paragraph, will be observed again, with the formation of AABW in the Weddell Sea starting again.

These two POP-patterns describe the rotation of a dipole anomaly in the yz-plane with the vector of rotation pointing to the west. The upper pole moves northward with the surface waters of the Atlantic. The anomalies are amplified in the Southern Ocean. This pattern is very similar to the oscillator described by Mikolajewicz and Maier-Reimer (1990) with a composite analysis. They give a value of 320 years for the period of this process, which is not significantly different from the 330 years obtained with the POP-analysis.

The proportion of variance explained by this pattern is typically more than 70% in the Atlantic, but significantly lower around 1000m depth (not shown). In the Southern Ocean the fraction of the total variance explained by the POP is only about 40%.

The time series of the amplitude of the complex POP-coefficients (fig. 7) reveals that there are two discrete modes of operation for the oscillator, either 'on' (with values of about 0.2) or 'off'. Values in between are almost absent and most of them can be attributed to transition periods between the two modes. In the 'on'-mode (years 500 to 1550, 1900 to 2400 and 3250 to the end of the integration), the phase velocity is almost constant through time. In the 'off'-mode the phase velocity is more irregular, but in periods before the transition to the 'on'-mode an almost constant phase velocity might be observed. The existence of the two discrete modes of operation is demonstrated in fig. 10 showing a scatterplot of the real and imaginary part of the POP-coefficients.

Another point of interest is the question of the behaviour of the salinity anomalies away from the previously described section through the Atlantic, and the behaviour of the oscillation in other variables. An analysis with associated correlation patterns (ACPs, defined by linear regression versus the two POP-coefficient time series) is appropriate to answer this question. The results of this analysis are two patterns a^I and a^R - each of them associated

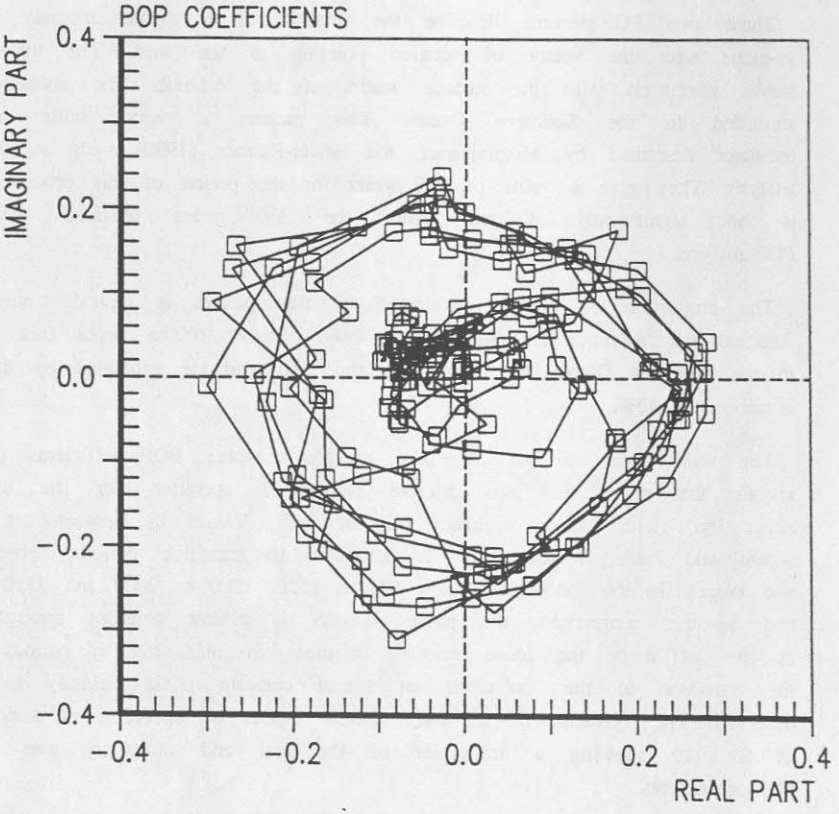

Fig. 10

Scatterplot of 20-year averages of the two components of the POP-coefficents. Consecutive pairs of data are connected by a line. The normal propagation of the pattern corresponds to a clockwise rotation on this plot.

with one POP-pattern - which can be interpreted the same way as the POP-patterns.

The ACPs of the near surface salinity are shown in fig. 11. The positive salinity anomaly in the southern Indian and Atlantic oceans - connected with the imaginary POP-pattern - invades the surface waters of the Atlantic and spreads northward while significantly losing strength. After about 80 years the surface waters of the Atlantic are all saltier than the mean (except for the Arctic). This holds true even another 80 years later, when the observed anomaly pattern is the negative of the pattern described first, the center has moved northward but at the coast of Antarctica a negative salinity anomaly has developed. The northward spreading into the Atlantic follows the upper branch of the mean thermohaline circulation of this ocean.

But there does exist another direction of propagation. The positive salinity anomaly with its maximum at the coast of Antarctica just south of Africa propagates in both(!) directions along the coast to the Ross Sea, where the anomaly reaches its maximum approximately 160 years later. Here the anomaly decays for about 100 years. This two-branch propagation to the Ross Sea, with one branch propagating against the direction of the ACC, was particularly surprising for us. Close to the coast of Antarctica the eastward velocity component is small (except in the Drake Passage) and at many locations the surface flow of the model is even westward in our model. The propagation of the salinity anomaly is accompanied by changes in the formation of bottom water. So the westward propagating branch does not necessarily mean an advection process but could be a secondary effect of the propagating deepwater formation. This part of the problem will need further investigation in future work.

Besides these two propagating patterns two almost standing oscillations in the east Pacific can be seen: a strong one centered at 30°S and a weaker one at 30°N. Both oscillators are completely out of phase.

The explained variance in the surface waters of the Atlantic is typically about 80%. In the ACC between 40 and 70% of the total variance is explained by these two patterns, although the two patterns have their maximal amplitudes in this region. Thus the relatively low values must be an effect of the high

noise level in the Southern Ocean due to strong fluctuations on a shorter time scale. The oscillation in the southeast Pacific explains up to 80% of the total variance, wherea the weaker counterpart in the northeast Pacific reaches maximal values of 45% explained variance.

The ACPs of the salinity in 2000m depth (see fig. 12) show the southward avdection of salinity anomalies from the northwest Atlantic in a deep western boundary current by the mean thermohaline circulation. In the Southern Ocean a moving pattern follows the coastline of Antarctica. The direction of propagation is eastward. In the pattern a^I the anomaly has its maximum at 60°E. 80 years later (in the pattern a^R) the maximum has reached 100°E. Another quarter period later, the maximum has reached the Ross Sea (pattern $-a^I$). On its route, side branches moving into the Indian and the Pacific Oceans can be seen.

The variance explained by these two patterns in the western Atlantic is about 70%. In the Southern Ocean this value is drastically reduced to about 20 to 60%.

6. Interpretation

From the results shown up to now, it becomes quite clear that the POP-analysis reveals one eigenmode of the ocean circulation. This eigenmode has been excited by the stochastic forcing. This mode has the structure of a dipole that is advected by the mean thermohaline circulation of the Atlantic. The time scale of this process is connected with the flushing time of the Atlantic, which can be estimated from the volume and the exchange rates of our OGCM at 30°S to be about 400 years. The small discrepancy between the two numbers might be explained by the relatively fast propagation in western boundary currents (both at the surface and in the deep Atlantic, cf. Stommel and Arons 1960).

The upper branch of the dipole moves northward with the surface waters of the Atlantic, and the deeper branch is advected southward in the outflowing North Atlantic deep water. In the region of the Southern Ocean the anomalies gain considerably in strength through the suppression of Antarctic bottom water formation. The following mechanism is responsible for the amplification.

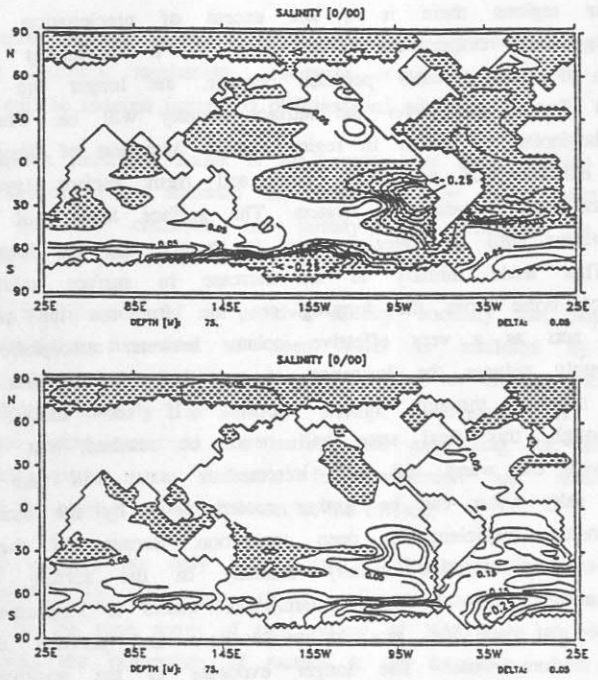

Fig. 11

Associated correlation patterns a^I and a^R of the near surface salinity (75m depth). Shading indicates negative values.

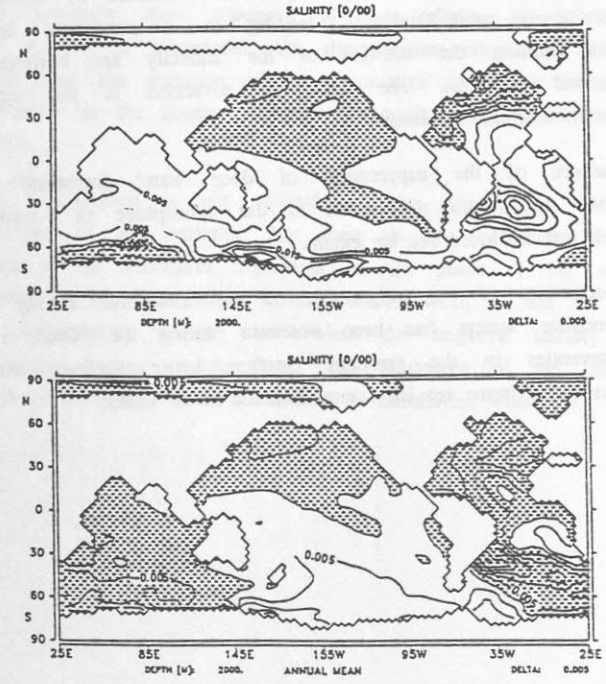

Fig. 12

Associated correlation patterns a^I and a^R of the salinity in 2000m depth. Shading indicates negative values.

In polar regions there is a net excess of precipitation and runoff from Antarctica over evaporation. This leads to a continuous reduction of the salinities of surface water particles because, the longer the water is exposed to these fluxes, the lower the surface salinity will be. The typical situation at the beginning of winter in regions where formation of deep water can occur is the existence of a relative cold and fresh surface layer over relatively warm and salty intermediate waters. The surface layer will be cooled down during winter until the freezing point is reached and the formation of sea ice starts. This leads initially to an increase in surface salinity due to the release of brine from the forming sea ice. But sea ice of more than 1m thickness acts as a very effective isolator between atmosphere and ocean and thus strongly reduces the formation of new sea ice and thus the increase in surface salinity through brine rejection. If the initial stratification is weak enough, this final state will never be reached, but instead convective mixing with the warm and salty intermediate water will take place. This now relatively salty water can be further cooled down by the atmosphere and thus reach densities sufficient for deep convection. Because of the presence of a sufficient strong negative salinity anomaly in the surface waters the first step of mixing with the salty intermediate waters is suppressed and finally a thick layer of sea ice acts as an isolator and prevents the formation of Antarctic bottom water. The longer exposure to the positive net freshwater flux at the surface and the absence of incorporation of the salty intermediate water lead to a strong amplification of the negative anomaly. This now even stronger negative salinity anomaly makes the formation of bottom water in the next year even more unlikely, leading to a permanent amplification. The mechanisms limiting the strength of the anomaly are horizontal and vertical advection and diffusion. The horizontal advection is the most effective of these negative feedback mechanisms.

Consequences of the suppression of deep water formation are significantly reduced heat loss from the ocean to the atmosphere in winter, lower surface temperatures and increased sea ice extent.

This mechanism of the suppression of the convective mixing between surface and intermediate waters has been observed during the 'Great salinity anomaly' of the seventies in the northern North Atlantic together with low surface temperatures and extreme sea ice extent (Dickson et al. 1988).

The negative salinity anomaly must exceed a certain strength to initiate this positive feedback mechanism, otherwise convection is not suppressed and the anomaly will be reduced further by diffusion and advection.

The mechanism described above is the reason why Bryan (1986) and Marotzke (1990) had difficulties to maintain the climate of the model after a switch in the surface boundary condition for salinity from relaxation to climatological surface salinity to the prescription of salt/freshwater fluxes.

A similar amplification of a positive salinity anomaly can happen in polar regions where the formation of deep water is inhibited by low surface salinities and by isolation of the water from the air through sea ice. If the positive salinity anomaly is strong enough, convection is initiated thus bringing more saline water to the surface and amplifying the anomaly making the conditions even more favorable for convection and reducing sea ice formation and the residence times of water at the surface.

The dipole anomaly not only is advected by the mean thermohaline circulation of the Atlantic, but also has strong influence on the circulation, as is demonstrated by the time series of the outflow of NADW to the Southern Ocean (fig. 5). During the occurrence of pattern $\mathfrak{R}$ the formation of Antarctic bottom water has its maximum (and so does the mass transport of the Antarctic circumpolar current) and the formation of NADW is relatively weak. The consequence is a slowing down of the thermohaline circulation of the Atlantic and thus a relatively slow transport of the salinity anomalies. While the formation of AABW is suppressed, the thermohaline circulation of the Atlantic is strong and thus the transport of the anomalies fast. The variations of the outflow of NADW to the Southern Ocean can reach values of 40% of the mean outflow of 17Sv.

The linear POP-method is not optimal for the investigation of nonlinearities in the behaviour of an oscillator, but there is an indication of this change of propagation of the anomalies dependent on the phase of the anomaly itself. The phase velocity usually reaches a minimum between 0 and 90°. This phase corresponds approximately to the time when the negative salinity anomaly in the deep Atlantic reaches its maximum. The behaviour of the rotation of the anomaly has some similarities to the rotation of an unbalanced wheel.

A strong simplification is the neglect of any kind of feedback with the atmosphere. In particular, the strength of the heat flux anomalies in the Southern Ocean means that strong atmospheric responses in both wind stress and surface temperature must be expected. This might cause an overestimation of the magnitude of the changes in the heat fluxes.

7. Sensitivity experiments

The sensitivity of the eigenmode to changes in the amplitude of the stochastic forcing is an important question. Two sensitivity experiments were carried out. The amplitude of the forcing is the only difference to the experiment described in the previous sections.

In a first sensitivity experiment the globally averaged standard deviation of the stochastic freshwater fluxes was reduced from 16mm/month to 5mm/month. The time series of the mass transport of the Antarctic circumpolar current (not shown) does not show the typical eigenoscillations with a timescale of 300 years (nor any other strong signal). The explanation is the fact that the salinity anomalies now cannot reach the threshold value to allow the positive feedback mechanism in the Southern Ocean to work.

In a second experiment the standard deviation of the noise was tripled from 16mm/month to 48mm/month standard deviation. In this experiment there was a drastic climate drift that prevented the investigation of the reaction of the oscillator to this increased amplitude of the forcing. In year 400 of this experiment, there was a transition to the other mode of the thermohaline circulation of the Atlantic. The negative salinity anomalies in the North Atlantic had reached a strength that the amplification process was excited in the North Atlantic leading to a permanent suppression of NADW formation and a reversal of the thermohaline circulation of the Atlantic. The behaviour is very similar to the response of the ocean circulation to glacier melting as investigated by Mikolajewicz and Maier-Reimer (1989). The transition was not reversed in the next 1600 years of the simulation. The strength of the climate drift prevented the proper analysis of this experiment.

The dependence of the oceanic response to perturbation freshwater fluxes is highly nonlinear with respect to the amplitude of the perturbation.

The dependency of the performance of the oscillator on the formulation of the equation of state was investigated in two additional experiments. In a first experiment the density was computed with respect to surface pressure rather than actual pressure, thus ignoring all effects connected with the compressibility of sea water. These compressibility effects are essential for the type of oscillators proposed by Müller and Willebrand (1985). The oscillation occurred in this experiment as well, but with slightly reduced period, an effect that can be explained by the increased outflow of NADW in this experiment (21 Sv compared to 17 Sv in the standard run with stochastic forcing).

In another sensitivity experiment a linear equation of state[6] was used. In this experiment the eigenmode did not occur. Thus the oscillator described in this paper cannot be of the type proposed by Müller and Willebrand (1985) but the nonlinearity of the equation of state seems to be important anyhow.

8. Comparison with data

An important question is whether this eigenmode occurs in the real ocean. If so, the simulated variations in the ocean-atmosphere heat exchange at high latitudes should be detectable in climatic records. Unfortunately, the sparseness of the data prevents a real validation of the model results.

Detailed and very long records are available for $\delta O18$ from ice cores, a proxy index which is correlated with annual mean temperature. One must be careful, however, with directly interpreting these values as temperature signals, because there are several other factors that can influence this quantity. Fisher (1982) compared two $\delta O18$ records of 5300 years length from Arctic ice cores 600 km apart to remove local effects. He reported peaks in the coherence spectra at periods of 2500, 625, 417, 330 and 185 years. The exact location of the spectral peaks is, of course, ambiguous. Dansgaard et al. (1971) analyzed the oxygen isotope record from the Camp Century ice core (Greenland) and found a dominating signal with a period about 350 years.

---

[6] linearized around 3°C, 35 °/₀₀ and surface pressure.

From existing long-term data records we can only conclude that there is indeed some variability in the frequency ranges discussed here. But whether this is related to the pattern described here is impossible to decide from the available data.

9. Conclusion

In an OGCM forced with white-noise fresh water fluxes, the internal dynamics of the ocean strongly influence the variability on time scales longer than a few decades. The most pronounced example of this variability is a dipole anomaly advected by and interacting with the mean thermohaline circulation of the Atlantic, with a mean advection period of 330 years. The occurrence of these oscillations strongly depends on the amplitude of the stochastic forcing. We suggest that oscillations of this type may contribute significantly to natural climatic variability on time scales of centuries.

ACKNOWLEGDEMENTS

We appreciate discussions with Klaus Hasselmann. We gratefully acknowledge the assistance of Jörg Wolff and Peter Wright in carefully reading this manuscript and Marion Grunert for drawing the figures.

REFERENCES:

Baumgartner, A. and E. Reichel (1975). Die Weltwasserbilanz. Oldenbourg Verlag München, 179p.

Berger, W.H. and E. Vincent (1986). Sporadic Shutdown of North Atlantic deep water production during the Glacial-Holocene transition? *Nature* **315**, 53-55.

Broecker, W.S., M. Andree, W. Wolfli, H. Oeschger, G. Bonani, J. Kenett and D. Peteet (1988). The chronology of the last deglaciation: implications to the cause of the Younger Dryas event. *Paleoceanography* **3**, 1-19.

Broecker, W.S., G. Bond, M. Klas, G. Bonani and W. Wolfli (1990). A Salt Oscillator in the Glacial Northern Atlantic? *Paleoceanography* **5**, 469-477.

Bryan, F. (1986). High latitude salinity effects and interhemispheric thermohaline circulations. *Nature* **305**, 301-304.

Cox, M. (1975). A baroclinic Numerical Model of World Ocean. In *Numerical Models of Ocean circulation*, National Academy of Sciences, Washington, 107-120.

Crowley, T.J. and G.R. North (1991). Paleoclimatology. Oxford University Press, New York, 335p.

Cubasch, U., K. Hasselmann, H. Höck, E. Maier-Reimer, U. Mikolajewicz, B.D. Santer and R. Sausen (1991). Time-dependent greenhouse Warming Computations with a Coupled Ocean-Atmosphere Model. *Climate Dyn.* (subm.).

Dansgaard, W., S.J. Johnsen, H.B. Clausen, C.C. Langway (1971). Climatic record revealed by the Camp Century ice core.In: K.K. Turekian (ed.), The Cenozoic Glacial Ages. Yale University Press, New Haven, Conn., 37-56.

Dansgaard, W., S.J. Johnsen, H.B. Clausen, D. Dahl-Jensen, N. Gundestrup and C.U. Hammer (1984). North Atlantic climatic oscillations revealed by deep Greenland ice cores. In J.E. Hansen and T. Takahashi (eds.), Climate Processes and Climate Sensitivity, AGU Geophysical Monograph 29, Washington DC.

Dickson, R.R., J. Meincke, S.-A. Malmberg and A.J. Lee (1988). The "Great Salinity Anomaly" in the Northern North Atlantic 1968-1982. *Prog. Oceanog.* **20**, 103-151.

Fisher, D.A. (1982). Carbon-14 production compared to oxygen isotope records from Camp Century, Greenland and Devon Island, Canada. *Climatic Change* **4**, 419-426.

Folland, C.K., T.R. Karl and K.Y. Vinnikow (1990). Observed Climate Variations and Change. In J.T. Houghton, G.J. Jenkins and J.J. Ephraims (eds.) *Climate Change*. Cambridge University Press, Cambridge, 198-238.

Frankignoul, C. and K. Hasselmann (1977). Stochastic climate models, part II: Application to sea-surface temperature anomalies and thermocline variability. *Tellus* **29**, 289-305.

Gates, W.L. (1985). Modelling as a means of studying the climate system. In M.C. Mac Cracken and F.M. Luther (eds.) Projecting the climatic effects of increasing carbon dioxide. Department of Energy DOE/ER-0237, Washington DC, 57-79.

Gordon, A.L. (1986). Interocean Exchange of Thermocline Water. *J. Geophys. Res.* **91**, 5037-5046.

Gordon, A.L. and A.R. Piola (1983). Atlantic Ocean upper layer salinity budget. *J. Phys. Oceanogr.* **13**, 1293-1300.

Hasselmann, K. (1976). Stochastic climate models, Part I, Theory. *Tellus* **28**, 6, 473-485.

Hasselmann, K. (1979). On the signal-to-noise problem in atmospheric response studies. *Meteorology of Tropical Oceans*, Royal Met. Soc. 251-259.

Hasselmann, K. (1982). An ocean model for climate variability studies. *Prog. Oceanog.* **11**, 69-92.

Hasselmann, K. (1988). PIPs and POPs: The reduction of Complex Dynamical Systems Using Principal Interaction and Oscillation Patterns. *J. Geophys. Res.* **93**, D9, 11015-11021.

Hellermann, S. and M. Rosenstein (1983). Normal monthly wind stress data over the world ocean with error estimates. *J. Phys. Oceanogr.* **13**, 1093-1104.

Herterich, K. and K. Hasselmann (1987). Extraction of Mixed Layer Advection Velocities, Diffusion coefficients, Feedback Factors and atmospheric forcing Parameters from the Statistical Analysis of North Pacific SST Anomaly Fields. *J. Phys. Oceanogr.* **17**, 2145-2156.

Humboldt, A. von (1845). Kosmos. Entwurf einer physischen Weltbeschreibung. Erster Band. Stuttgart and Tübingen, 453 p.

Lamb, H.H. (1977). Climate: present past and future. Vol. 2. Methuen & Co London, 835 p.

Levitus, S. (1982). Climatological Atlas of the World Ocean. NOAA Professional Paper 13, Rockville Md.

Lemke, P. (1977). Stochastic climate models, part 3, application to zonally averaged energy models. *Tellus* **29**, 385-392.

Lemke, P., E.W. Trinkl and K. Hasselmann (1980). Stochastic Dynamic Analysis of Polar Sea Ice Variability. *J. Phys. Oceanogr.* **10**, 2100-2120.

Maier-Reimer, E. and K. Hasselmann (1987). Transport and storage of CO_2 in the ocean - an inorganic ocean-circulation carbon cycle model. *Climate Dyn.* **2**, 63-90.

Maier-Reimer, E. and U. Mikolajewicz (1989). Experiments with an OGCM on the cause of the Younger Dryas. in A. Ayala-Castanares, W. Wooster and A. Yanez-Arancibia (eds.) *Oceanography 1988*. UNAM Press Mexico D.F., 87-100.

Maier-Reimer, E., U. Mikolajewicz and K. Hasselmann (1991). On the sensitivity of the global ocean circulation to changes in the surface heat flux forcing. *J. Phys. Oceanogr.* (subm.).

Manabe, S. and R.J. Stouffer (1989). Two stable equilibria of a coupled ocean-atmosphere model. *Journal of Climate* **1**, 841-866.

Marotzke, J. (1990). Instabilities and Multiple Equilibria of the Thermohaline Circulation. Berichte aus dem Institut für Meereskunde Nr. 194, Kiel, 126 p.

Marotzke, J., P. Welander and J. Willebrand (1988). Instability and multiple steady states in a meridional-plane model of the thermohaline circulation. *Tellus* **40A**, 162-172.

Mikolajewicz, U. and E. Maier-Reimer (1990). Internal secular variability in an OGCM. *Climate Dyn.* **4**, 145-156.

Müller, P. and J. Willebrand (1985). Compressibility effects in the thermohaline circulation: a manifestation of the temperature-salinity mode. *Deep-Sea Res.* **33**, 559-571.

Rasmusson, E.M. and T.H. Carpenter (1982). Variations in tropical sea surface temperature and surface wind fields associated with the Southern Oscillation/El Niño. *Mon. Weather Rev.* **110**, 354-384.

Reynolds, R.W. (1979). A stochastic forcing model of sea surface temperature anomalies in the North Pacific and North Atlantic. Clim. Res. Inst., Rep. 8, Oregon State University, Corvallis.

Roemmich, D. and C. Wunsch (1985). Two transatlantic sections: meridional circulation and heat flux in the subtropical North Atlantic Ocean. *Deep-Sea Res.* **32**, 619-664.

Rooth, C. (1982). Hydrology and ocean circulation. *Progr. Oceanogr.* **11**, 131-149.

Stommel, H. (1961). Thermohaline convection with two stable regimes of flow. *Tellus* **13**, 224-230.

Stommel, H. and A.B. Arons (1960). On the abyssal circulation of the world ocean - II. An idealized model of the circulation pattern and amplitude in oceanic basins. *Deep-Sea Res.*, **6**, 217-233.

Storch, H. von, T. Bruns, I. Fischer-Bruns and K. Hasselmann (1988). Principal Oscillation Pattern analysis of the 30-60 day oscillation in a GCM equatorial troposphere. *J. Geophys. Res.* **93**, 11015-11022.

Storch, H. v., G. Bürger, R. Schnur, and J.-S. Xu, (1991). POP art. This volume.

Stouffer, R.J., S. Manabe and K. Bryan (1989). Interhemispheric asymmetry in climate response to a gradual increase of atmospheric CO_2. *Nature* **342**, 660-662.

Welander, P. (1986). Thermohaline effects in the ocean circulation and related simple models. In J. Willebrand and D.L.T. Anderson (eds.) Large-Scale Transport Processes in Oceans and Atmospheres, D. Reidel, 163-200.

Whitworth, T. and R.G. Peterson (1985). Volume Transport of the Antarctic Circumpolar Current from Bottom Pressure Measurements. *J. Phys. Oceanogr.* 15, 810-816.

Wigley, T.M.L. and S.C.B. Raper (1990). Natural variability of the climate system and detection of the greenhouse effect. *Nature* 344, 324-327.

Wolff, J.-O., E. Maier-Reimer and D.J. Olbers (1991). Wind-driven flow over topography in a zonal β-plane channel: A quasigeostrophic model of the Antarctic Circumpolar Current. *J. Phys. Oceanogr.* 21, 236-264.

Woodruff, S.D., R.J. Slutz, R.L. Jenne and P.M. Steurer (1987). A comprehensive ocean-atmosphere data set. *Bull. Am. Meteorol. Soc.* 68, 1239-1250.

Wüst, G. (1933). Schichtung und Zirkulation des Atlantischen Ozeans. Das Bodenwasser und die Gliederung der Atlantischen Tiefsee. In Wissenschaftliche Ergebnisse der Deutschen Atlantischen Expedition auf dem Forschungs- und Vermessungsschiff "Meteor" 1925-1927, 6, 1. Teil.